HHS Public Access

Author manuscript

Anal Chem. Author manuscript; available in PMC 2024 July 16.

Published in final edited form as:

Anal Chem. 2023 January 17; 95(2): 1159–1168. doi:10.1021/acs.analchem.2c03897.

Sensitive and Quantitative Point-of-Care HIV Viral Load Quantification from Blood Using a Power-Free Plasma Separation and Portable Magnetofluidic Polymerase Chain Reaction Instrument

Hoan T. Ngo,
Department of Mechanical Engineering, Johns Hopkins University, Baltimore, Maryland 21218, United States

Mei Jin,
Department of Biomedical Engineering, Johns Hopkins University, Baltimore, Maryland 21218, United States

Alexander Y. Trick,
Department of Biomedical Engineering, Johns Hopkins University, Baltimore, Maryland 21218, United States

Fan-En Chen,
Department of Biomedical Engineering, Johns Hopkins University, Baltimore, Maryland 21218, United States

Liben Chen,
Department of Mechanical Engineering, Johns Hopkins University, Baltimore, Maryland 21218, United States

Kuangwen Hsieh,
Department of Mechanical Engineering, Johns Hopkins University, Baltimore, Maryland 21218, United States

Tza-Huei Wang
Department of Mechanical Engineering and Department of Biomedical Engineering, Johns Hopkins University, Baltimore, Maryland 21218, United States; Institute for NanoBioTechnology, Johns Hopkins University, Baltimore, Maryland 21218, United States

Corresponding Author Tza-Huei Wang – Department of Mechanical Engineering and Department of Biomedical Engineering, Johns Hopkins University, Baltimore, Maryland 21218, United States; Institute for NanoBioTechnology, Johns Hopkins University, Baltimore, Maryland 21218, United States; thwang@jhu.edu.

Author Contributions

The manuscript was written through contributions of all authors. All authors have given approval to the final version of the manuscript.

The authors declare no competing financial interest.

ASSOCIATED CONTENT

Supporting Information

The Supporting Information is available free of charge at https://pubs.acs.org/doi/10.1021/acs.analchem.2c03897.

Design and dimension of the plasma separation device; the effect of absorbent capacity to plasma separation efficiency; instrument's block diagram and picture; virus recovery of plasma separation; the effect of lysis/binding time; comparison with commercial nucleic acid extraction kits; LOD of HIV-1 RNA quantification assay; and plasma separation device: device-to-device variation (PDF)

Plasma separation procedure (MP4)

Abstract

Point-of-care (POC) HIV viral load (VL) tests are needed to enhance access to HIV VL testing in low- and middle-income countries (LMICs) and to enable HIV VL self-testing at home, which in turn have the potential to enhance the global management of the disease. While methods based on real-time reverse transcription-polymerase chain reaction (RT-PCR) are highly sensitive and quantitatively accurate, they often require bulky and expensive instruments, making applications at the POC challenging. On the other hand, although methods based on isothermal amplification techniques could be performed using low-cost instruments, they have shown limited quantitative accuracies, i.e., being only semiquantitative. Herein, we present a sensitive and quantitative POC HIV VL quantification method from blood that can be performed using a small power-free three-dimensional-printed plasma separation device and a portable, low-cost magnetofluidic real-time RT-PCR instrument. The plasma separation device, which is composed of a plasma separation membrane and an absorbent material, demonstrated 96% plasma separation efficiency per 100 μL of whole blood. The plasma solution was then processed in a magnetofluidic cartridge for automated HIV RNA extraction and quantification using the portable instrument, which completed 50 cycles of PCR in 15 min. Using the method, we achieved a limit of detection of 500 HIV RNA copies/mL, which is below the World Health Organization's virological failure threshold, and a good quantitative accuracy. The method has the potential for sensitive and quantitative HIV VL testing at the POC and at home self-testing.

Graphical Abstract

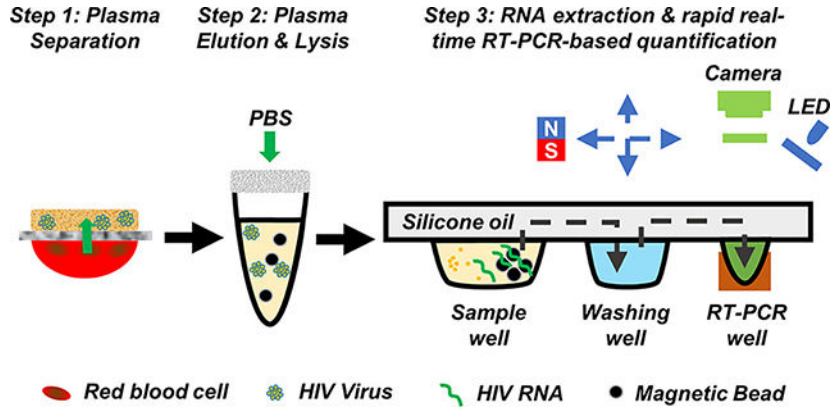

INTRODUCTION

More than 40 years since the first case was reported in 1981, HIV/AIDS has claimed an estimated 36.3 million lives and is one of the deadliest infectious diseases worldwide.[1] In 2020 alone, an estimated 680,000 people died from AIDS-related illness.[1] About 37.7 million people are living with HIV/AIDS globally, with more than half living in Eastern and Southern Africa.[2–4] Although no cure for HIV/AIDS has been developed, antiretroviral therapy (ART) can suppress HIV viral load (VL) to undetectable concentrations, which effectively means that the infection is untransmittable.[5–8] About ~28.2 million people living with HIV/AIDS in the world are receiving ART.[1] HIV VL testing is an important tool to monitor ART treatment efficacy and guide clinical action.[9–13]

Commercial HIV VL test kits based on real-time reverse transcription-polymerase chain reaction (RT-PCR) such as the Abbott RealTime HIV-1 and the Roche Cobas AmpliPrep/TaqMan HIV-1 are sensitive with limits of detection (LODs) of 20–50 HIV RNA copies/mL[14–18] but require expensive instruments and highly trained personnel. Therefore, these kits have been confined to central laboratories. In sub-Saharan Africa, where most HIV/AIDS patients live and where testing infrastructure is limited, central laboratory-based testing suffers from long turnaround times of a few months, on average.[19,20] Long turnaround time is a cause of delay of care and loss to follow-up, which in turn contribute to poor treatment outcome and the spread of HIV drug resistance.[4,21–24] Improving access to HIV/AIDS diagnosis and HIV VL testing in low- and middle-income countries (LMICs) is important to achieve the UNAIDS 95–95-95 targets (i.e., diagnose 95% of all HIV-positive individuals, provide ART for 95% of those diagnosed, and achieve viral suppression for 95% of those treated) set for 2030.[24]

Recently, several research studies have shown that the usage of near point-of-care (POC) HIV VL testing platforms such as Cepheid's GeneXpert and Abbott's m-PIMA in seven sub-Saharan African countries and South Africa significantly reduced turnaround time, shortened time to clinical action, and improved retention in care and treatment outcome.[20,25] However, these instruments require constant electricity, cost $17,500 and $25,000, respectively, and use single-use test cartridges with prices >$25.[26] Furthermore, both platforms require plasma as the starting sample for quantitative output,[27–31] the isolation of which is challenging at the POC. Thus, these platforms may be more suited for HIV VL testing in clinic-based settings. Meanwhile, the SAMBA HIV-1 Semi-Q Test whole blood assay can use whole blood as the starting sample by using a proprietary leukodepletion column but is only semiquantitative, i.e., does not provide a specific VL number.[32,33] There is an unmet need for POC HIV VL testing platforms from blood that are rapid, affordable, simple to use, sensitive, and quantitatively accurate for community-based settings and at home self-testing.

Several efforts have been made to develop such a POC HIV VL test.[4,34–40] For example, Kadimisetty et al. reported a three-dimensional (3D)-printed sample concentrator for plasma separation, HIV virus lysis, and HIV nucleic acid enrichment at the POC.[35] However, the samples had to be transported to centralized laboratories for manual washing and VL quantification using benchtop PCR machines. Phillips et al. reported a POC HIV nucleic acid testing (NAT) device called microRAAD to detect HIV from whole blood using RT-LAMP isothermal amplification.[36] However, the LOD was quite high, 2.3×10^7 virus copies/mL of whole blood, and, with a low quantitative accuracy, the platform is more suited for yes/no detection rather than VL quantification. Also, using RT-LAMP, Liu et al. reported a USB-interfaced POC HIV VL testing device from blood with a LOD of ~214 viral RNA copies/mL of whole blood.[37] Although the device is compact and sensitive, since blood samples spiked with already extracted HIV RNA were used for the LOD experiment, it is unclear what LOD the device will achieve with blood samples containing HIV viruses. Furthermore, with an R^2 of 0.85 upon linear fitting the standard curve and large standard deviations, the device is more suited for semiquantitative tests (i.e., differentiating between high, medium, and low viral loads). Hull et al. reported the use of an HIV RPA assay and a target-mimicking internal amplification control that could distinguish ≥10-fold

differences in HIV RNA copy numbers from the World Health Organization (WHO) treatment failure threshold.[38] However, the method is also semiquantitative and does not include sample preparation. Wang et al. reported a digital format of isothermal nucleic acid sequence-based amplification (NASBA) for quantifying HIV-1 RNA and achieved better quantitative accuracy and sensitivity than real-time NASBA.[39] Although quantitative and sensitive, digital format increases complexity regarding chip fabrication, sample loading, and instrumentation. Among techniques for quantifying nucleic acid copy number in a single bulk reaction, real-time RT-PCR has better quantitative accuracy than isothermal techniques.[38,41] Nevertheless, real-time RT-PCR requires bulky and expensive instruments due to the need of thermal cycling and fluorescence readout.[42] Several research groups have attempted to develop low-cost and portable real-time RT-PCR instruments for applications at the POC.[43–47] We previously reported a filtration-assisted HIV VL quantification method based upon a portable magnetofluidic real-time RT-PCR platform with a LOD of 1000 copies using 10 μL of whole blood, i.e., 100,000 copies/mL of blood and a good quantitative accuracy.[40] However, the WHO defines ≥1000 HIV RNA copies/mL as the threshold for virological failure, while some other public health authorities use lower thresholds (e.g., ≥200 copies/mL).[48,49] Therefore, to be able to detect virological failure, a platform must achieve a LOD of 1000 HIV RNA copies/mL or lower.

To accomplish this, in this work, we developed a novel, power-free plasma separation method and device that can process 10 times larger volume of whole blood (i.e., 100 μL of whole blood). We then coupled it with an enhanced RNA extraction and quantification protocol in a magnetofluidic cartridge. The plasma separation device was composed of a plasma separation membrane and an absorbent material housed in a small 3D-printed casing. Using the device, 96% of the available plasma could be separated from 100 μL of whole blood after 3 min. After an elution step using phosphate-buffered saline (PBS), plasma solution was obtained in a tube. A lysis/binding buffer solution and silica-coated magnetic beads were added to the tube for HIV virus lysing and HIV RNA capturing. The lysate was then transferred into a magnetofluidic cartridge for automated nucleic acid extraction and quantification using a portable and low-cost magnetofluidic real-time RT-PCR instrument (Figure 1). The instrument has a rapid thermocycling design that can complete 50 PCR cycles in 15 min. Using the method, we were able to quantify HIV VL from 100 μL of blood with a LOD of 500 HIV RNA copies/mL and a good quantitative accuracy (R^2 of 0.97 upon linear fitting the standard curve). The total turnaround time was ~45 min. This method therefore has the potential for sensitive and quantitative HIV VL quantification and virological failure detection from blood at the POC and at home self-testing.

EXPERIMENTAL SECTION

Design and Fabrication of the Plasma Separation Device.

The plasma separation device was designed using Fusion 360 (Autodesk). Detailed dimensions can be found in Figure S1. The design was 3D printed using a Form 2 3D printer (Clear Resin, Formlabs). Absorbent discs of an A/D glass fiber filter (thickness 660 μm, Pall Corporation) with a diameter of 8.5 mm were prepared using a hole puncher. Absorbent discs of blotting paper (grade 703, thickness 380 μm, VWR) with a diameter

of 13 mm were prepared using another hole puncher. Absorbent discs of an A/D glass fiber and blotting paper were attached to the absorber module of the plasma separation device using a double-sided adhesive ring (Figure S1). Discs of a Vivid plasma separation membrane (grade GR, thickness 330 μm, Pall Corporation) with a diameter of 15.875 mm were prepared using a 5/8 inch hole puncher. The Vivid plasma separation membrane disc was attached to the filter module of the plasma separation device using two double-sided adhesive rings with the shiny side of the membrane facing up (Figure S1).

Plasma Separation.

To conduct plasma separation, the absorber module, which holds the absorbent discs, was twisted and locked with the filter module, which holds the Vivid plasma separation membrane disc, bringing the absorbent discs into contact with the plasma separation membrane (Figure 2A). Then, 100 μL of whole blood spiked with 1 μL of HIV viral particles (AcroMetrix HIV-1 Panel copies/mL, Microgenics Corporation) was loaded onto the bottom side of the Vivid plasma separation membrane. The device was put aside upright for 3 min so that plasma could wick through the membrane and into the absorbent discs. The absorber module with the absorbent discs still attached was removed from the filter module. A syringe preloaded with 500 μL of PBS 1× (Gibco) was inserted into the absorber module to flush out the plasma absorbed in the absorbent discs into a collection tube. Video S1 shows the entire procedure of plasma separation using the proposed plasma separation method.

Fabrication of the Magnetofluidic Cartridge.

The magnetofluidic cartridge was designed and assembled, as previously described.[40] Briefly, the cartridge was designed with one sample well that can hold up to 500 μL of sample solution, a washing well that can hold up to 50 μL of washing solution, and a PCR well that can hold 7.5 μL of RT-PCR reaction mix solution. Cartridges were fabricated by thermoforming a polyethylene terephthalate glycol (PETG) film (Welch Fluorocarbon) onto 3D-printed molds using a vacuum-forming machine (JINTAI). Spacers were prepared by laminating a double-sided tape onto both sides of a 0.75 mm thick plastic sheet, followed by laser cutting. Spacers were then attached onto the thermoformed cartridges.

RT-PCR reaction mix solutions were prepared by mixing RT-PCR master mix (TaqMan Lyo-ready 1-Step RT-qPCR, Applied Biosystems, 1 μM final conc.), forward primers (5′-CATGTTTTCAGCATTATCAGAAGGA-3′, IDT, 1 μM final conc.), reverse primers (5′-TGCTTGATGTCCCCCCACT-3′, IDT, 1 μM final conc.), probe (5′FAM-CCACCCCACAAGATTTAAACACCATGCTAA-Q 3′, IDT, 0.25 μM final conc.), bovine serum albumin (New England Biolabs, 1 μM final conc.), Tween-20 (0.1% v/v final conc.), and DEPC-treated water (Quality Biological). The HIV-1 primers and probe sequences were adopted from an HIV-1 real-time RT-PCR assay with single-copy sensitivity previously developed by Palmer et al.[50] Solutions of 7.5 μL of RT-PCR reaction mix and 50 μL of washing solution (PEG 6000 (Sigma-Aldrich) 20% w/v Tween-20 (Sigma-Aldrich) 0.5% v/v in DEPC water) were loaded into the PCR well and washing well, respectively, of thermoformed cartridges with spacers attached.

Caps were prepared by laser cutting 1.5 mm acrylic plate (8560K171, McMaster-Carr) pre-laminated with polytetrafluoroethylene (PTFE) (6305A18, McMaster-Carr) on one side. After the reagent loading, as described above, cartridges were capped using the prepared caps with the PTFE-laminated side facing inside. Silicone oil 100 cSt (Sigma-Aldrich, 600 μL) was loaded into the cartridges to form fluid bridges between the sample well, washing well, and PCR well. Melted docosane wax (Sigma-Aldrich, 40 μL) was finally added and left to cool to room temperature to form a wax plug that would seal off the sample well and keep all reagents and silicone oil from moving. Prepared cartridges were kept on ice until use.

Portable Magnetofluidic Real-Time RT-PCR Instrument.

To transfer magnetic beads between the cartridge's sample well, washing well, and PCR well for nucleic acid extraction and quantification, a portable magnetofluidic real-time RT-PCR instrument[40] was used. The instrument had a two-dimensional (2D) magnetic arm that could move magnetic beads between the sample well, washing well, and PCR well of the cartridge. It also had a rapid thermocycling design.[45] The rapid thermocycler was based on a thermoelectric element (Peltier mini module, Custom Thermoelectric). One side of the thermoelectric element was epoxied to a mini-PCR heat block machined from 145 copper. The other side of the thermoelectric element was epoxied to a heatsink attached to a 5 V fan (Sunon). The temperature of the mini-PCR heat block was monitored by a thermistor probe (GA100K6MCD1, TE Connectivity) epoxied to the heat block. After a cartridge was inserted into the instrument, a resistive heater (Riedon PF1262–5RF1)-based heat block and the thermocycler were mounted under the sample well and the PCR well, respectively, of the cartridge by a motor (herein referred to as the mounting motor). The resistive heater was turned on to melt the wax plug, allowing the transfer of magnetic beads to the washing well and then the PCR well by the 2D magnetic arm. After an elution step in the PCR well, the magnetic beads were transferred out of the PCR well, and the thermocycler was turned on for rapid RT-PCR. Real-time fluorescence imaging was achieved via a 3-color RGB LED (Vollong), a focusing lens (10356, Carclo), a dual-band excitation filter (59003m, Chroma), a dual-band emission filter (535–700DBEM, Omega Optical), and a Raspberry Pi camera (Pi NoIR Camera V2, Raspberry Pi). The instrument was controlled by an Arduino Nano and a Raspberry Pi 3B+ computer, which communicate to each other via UART. The Arduino Nano controlled the 2D magnetic arm, the mounting motor, the 5 V fan, and the LED. The Raspberry Pi 3B+ computer controlled the camera and the resistive heater and the thermoelectric element (via motor driver shield dual TB9051FTG, Pololu). The block diagram of the instrument is shown in Figure S2.

Analytical Sensitivity of the HIV-1 RNA Real-Time RT-PCR Assay.

Analytical sensitivity of the HIV-1 RNA real-time RT-PCR assay was determined by spiking 1 μL of 10-fold serial dilutions (10^4–10^0 copies/μL) of synthetic HIV RNA sequences (VR-3245SD, ATCC) into 6.5 μL of RT-PCR reaction mix, which resulted in 10^4–10^0 copies/reaction final concentrations. Real-time RT-PCR were run using a benchtop Bio-Rad real-time PCR instrument and a rapid RT-PCR protocol (5 min RT at 50 °C, 10 s 95 °C hot start, and 50 cycles of denaturation at 95 °C for 1 s and annealing and extension at 60 °C for 1 s).

LOD Using Whole Blood Samples.

Samples for LOD analysis were prepared by spiking 1 μL of HIV viral particles (AcroMetrix HIV-1 Panel copies/mL, Microgenics Corporation) into 99 μL of HIV-1-negative whole blood samples (Interstate Blood Bank, Inc.) to 50,000 HIV RNA copies/mL, 5000 HIV RNA copies/mL, 500 HIV RNA copies/mL, and 0 HIV RNA copies/mL final concentrations. Plasma was separated, as described above. The collected plasma was mixed with 450 μL of lysis buffer (4 M GuSCN, 55 mM Tris–HCl, 25 mM EDTA, and 0.5% Triton X-100)[51] + 2 μL of carrier RNA (Applied Biosystems) + 2.25 μL of 2-mercaptoethanol (Sigma-Aldrich) + 4.5 μL of Proteinase K (Invitrogen) + 3 μL of silica-coated magnetic beads (MagBinding Beads, Zymo). To reduce the turnaround time, the mixture was incubated at room temperature for 5 min under shaking. After incubation, the mixture tubes were placed on a magnetic rack and 600 μL of the supernatant was removed. The remaining solutions (about 300 μL) were loaded into sample wells of cartridges preloaded with reagents, silicon oil, and docosane wax plug, as described above. The cartridges were inserted into the portable magnetofluidic real-time RT-PCR instrument (Figure S3) for wax plug melting (100 °C for 80 s), washing (15 round trips up and down), and elution (55 °C for 5 min). The magnetic beads were then moved out of the PCR well, and real-time RT-PCR was started (RT step, 55 °C for 5 min; PCR step, 50 cycles of denaturation at 100 °C for 2 s and annealing and extension at 55 °C for 2 s). The turnaround time of the entire workflow was ~45 min in which 50 PCR cycles took ~15 min. The LOD was determined as the lowest concentration in whole blood that resulted in successful detection of Cq in three independent experiments conducted on different days.

Statistical Analysis.

One-way ANOVA (multiple comparisons test of Tukey) was used to determine if there are any statistically significant differences between the means of different experimental conditions.

RESULTS AND DISCUSSION

Working Principle.

The working principle of our proposed HIV VL quantification method is illustrated in Figure 1, and the workflow includes the following steps: (1) The user loads a finger-prick volume of whole blood (100 μL) containing HIV viral particles onto the bottom side of a plasma separation membrane and waits for 3 min. Red blood cells, which are larger than the membrane's pore size, are blocked by the membrane, while plasma and HIV viral particles pass through and become absorbed into the absorbent material due to capillary force. (2) The user attaches the absorbent material onto the mouth of a tube and flushes the material with PBS using a syringe. Plasma and HIV viral particles are washed away from the absorbent material and fall into a solution of chaotropic salt-based lysis/binding buffer and silica-coated magnetic beads. HIV viral particles are lysed, and released HIV RNA are captured by the silica-coated magnetic beads. (3) The user transfers the lysate solution into the sample well of a cartridge (preloaded with RT-PCR reaction mix, washing buffer, and silicone oil) and inserts the cartridge into a portable instrument for automatic HIV RNA extraction and real-time RT-PCR quantification (Figures S2 and S3). First, the

magnetic beads are moved to a washing well for washing. Second, the magnetic beads are moved to a PCR well for direct elution of the HIV RNA into the RT-PCR reaction mix. Third, the magnetic beads are removed from the PCR well. Finally, a rapid thermocycler is mounted under the PCR well for amplification, and real-time quantification is achieved via fluorescence imaging using LEDs and a Raspberry Pi camera.

Plasma Separation Device.

Plasma is the gold-standard specimen for HIV VL quantification. Many efforts have been made to develop methods for plasma separation at the POC.[35,52–60] However, many of these methods are complex, have limited plasma separation efficiencies, and/or can only process small blood volumes. In response, we herein report a simple, power-free plasma separation method utilizing a Vivid plasma separation membrane and absorbent material. Figure 2 illustrates the plasma separation device that we developed. It was composed of two main parts: the absorber module, which held the absorbent material, and the filter module, which held the Vivid plasma separation membrane (Figure 2A). The two modules were attached together by a twist-and-lock mechanism. After whole blood was loaded (Figure 2B), the device was set aside in an upright position (Figure 2B inset) to allow for gravitational sedimentation of the red blood cells, thus reducing the issue of clogs in the plasma separation membrane and improving plasma separation efficiency. Three minutes later, the bottom surface of the plasma separation membrane appeared dry (Figure 2C). Meanwhile, the absorbent material changed to orange/pink color due to the absorbance of plasma (Figure 2D), as opposed to the white color at the beginning (Figure 2D inset). After eluting the absorbent material using a syringe preloaded with PBS (Figure 2E), plasma solution was collected in a tube, while the absorbent material's color returned to near-white color, indicating that most of the plasma was eluted (Figure 2E inset).

The amount of plasma absorbed into the absorbent material depends on two main factors: (1) contact between the absorbent material and the membrane and (2) absorbent capacity of the absorbent material. To ensure good contact between the absorbent material and the membrane, we designed the absorber module's height so that when the absorber module was twisted and locked into the filter module, a good contact between the absorbent material and the membrane was formed. Using this twist-and-lock mechanism, we expect to achieve better consistency regarding absorbent material–membrane contact than a previous design that relied on a screwing mechanism.[57] Absorbent capacity can be adjusted by varying the number of absorbent discs attached to the absorber module. The higher the number of absorbent discs, the higher the absorbent capacity, and therefore the higher the plasma separation efficiency (Figure 3). Plasma separation efficiency reached 96% ± 3% using 2 A/D glass fiber absorbent discs as opposed to 88% ± 11% using 1 A/D glass fiber absorbent disc and 63% ± 8% using no A/D glass fiber absorbent discs (see the Supporting Information for the separation efficiency calculation method). No statistically significant difference in plasma separation efficiency was found between 1 and 2 absorbent discs. Therefore, we decided to proceed with using two absorbent discs without further increasing the number of absorbent discs. The absorbed plasma was eluted from the absorbent discs using PBS, and a plasma solution was obtained. By quantifying the amount of virus in the

obtained plasma, we found ~32% HIV virus recovery in comparison to the gold-standard centrifuge-based method (Figure S4).

Nucleic Acid Extraction Protocol.

Once plasma was obtained from blood, HIV RNA needed to be extracted before real-time RT-PCR. The nucleic acid extraction step has been the bottleneck of implementing nucleic acid amplification tests (NAAT) at the POC and has attracted much research interest.[61–70,81] We previously reported a magnetofluidic cartridge approach that integrates automatic nucleic acid extraction and rapid real-time PCR in a single cartridge.[44,45] Our method has several advantages including (1) preloading of all required reagents in a cartridge, (2) ease of automation using low-cost off-the-shelf electronics components, (3) no requirement for fluidic manipulation, which in turn results in simple cartridge design and fabrication in addition to a small instrument footprint, and (4) integration of nucleic acid extraction and amplification in an enclosed cartridge, thus minimizing cross-contamination by amplicons from previous reactions.

With all the advantages, magnetic beads-based nucleic acid extraction in enclosed cartridges is challenging. Most published nucleic acid extraction protocols based on silica-coated magnetic beads and chaotropic salts chemistry involve several rounds of alcohol-based washing to remove inhibitors that would otherwise inhibit downstream amplification. Since alcohol itself is an inhibitor, after the last round of alcohol-based washing, magnetic beads must be air-dried to evaporate residual alcohol before the nucleic acid elution step. However, inside enclosed cartridges, air-drying is not amenable since magnetic beads are immersed in either aqueous phase or oil phase throughout the process. Nucleic acid extraction based on ChargeSwitch chemistry (Thermo Fisher) does not require alcohol washing and was used in cartridges by us and other groups.[44,45,71–75] However, for samples with a high content of protein, ChargeSwitch chemistry showed a lower recovery than silica-coated magnetic beads and chaotropic salts chemistry.[40,76] We and several groups reported the integration of silica-coated magnetic beads and chaotropic salts extraction chemistry into enclosed cartridges by replacing alcohol-based washing with PEG-based washing,[40] GuHCl-based washing,[77–79] or rapid water-based washing.[80]

In silica-coated magnetic beads and chaotropic salts extraction chemistry, sufficient lysis/binding time is needed for the silica-coated magnetic beads to capture nucleic acid released into lysate solution. In this work, we investigated the effect of lysis/binding time on the extraction yield. As we increased the lysis/binding time from 5 to 60 min, we observed decreasing Cq values, signaling improvements in the extraction yield (Figure S5). Although 60 min of lysis/binding time resulted in the lowest average Cq value, to keep a balance between the extraction yield and the assay time, we chose 30 min lysis/binding time to compare our HIV RNA extraction protocol with commercial RNA extraction kits.

On benchtop (SI, Section S6), our HIV RNA extraction protocol could achieve similar performance as the MagMAX Viral RNA Isolation Kit and the Zymo Quick-DNA/RNA Viral MagBead commercial kits (Figure 4 and Figure S6). Using a one-way ANOVA test (multiple comparisons test of Tukey), we found no statistically significant difference between Cqs by our extraction protocol and Cqs by the MagMAX and Zymo kits (Figure

4). Silica-coated magnetic beads and chaotropic salts extraction chemistry with PEG-based washing was therefore used in subsequent experiments involving HIV RNA extraction in a magnetofluidic cartridge.

Nucleic Acid Extraction in the Cartridge.

To extract nucleic acids using our magnetofluidic cartridge system, magnetic beads had to be moved from the sample well into the washing well using a permanent magnet. However, once the beads were in the washing well, without an active bead mixing mechanism, it was difficult to resuspend the magnetic beads into the solution, which is desirable for maximum washing efficiency. Adding a bead mixing mechanism would solve the issue but also adds complexity to the instrument. In this work, we found that washing efficiency in a cartridge could be improved by moving the beads up and down between the washing buffer solution and the silicone oil multiple times (Figure 5A). Higher round trip washes resulted in better washing efficiency (Figure 5B). For 1 round trip wash (i.e., 1 trip of beads moving down and up), no Cq could be detected, indicating that inhibitors remained on the beads and were carried over into the RT-PCR reaction mix. When the washing round trip number was increased to 5, the amplification signal could be detected. Further increasing the washing round trip number resulted in earlier Cqs, reaching the earliest Cq at 15 round trips. However, further increasing the number to 30 resulted in delayed Cq, possibly due to RNA loss from excessive washing. We therefore chose 15 washing round trips for subsequent experiments involving HIV RNA extraction in a magnetofluidic cartridge.

Sensitivity of the HIV-1 RNA Real-Time RT-PCR Assay.

To accurately quantify the extracted HIV-1 RNA, we used a rapid HIV-1 RNA real-time RT-PCR assay. Before integrating it into a cartridge, we evaluated the analytical sensitivity of the assay using 10-fold serial dilutions of synthetic HIV RNA sequences and benchtop equipment. The results showed single-copy sensitivity (Figure S7). We therefore chose this assay for integration into our cartridge system.

Limit of Detection Using Whole Blood Samples.

Finally, we conducted experiments encompassing the entire workflow from plasma separation from whole blood using the 3D-printed device to nucleic acid extraction and quantification using the portable magnetofluidic real-time RT-PCR instrument (Figures S2 and S3), and we evaluated the LOD of the method. HIV-1-negative whole blood samples (100 μL) spiked with HIV-1 viral particles to 50,000–0 HIV RNA copies/mL final concentrations were used. Triplicate experimental results showed that we could detect amplification curves at 50,000 copies/mL, 5000 copies/mL, and 500 copies/mL (Figure 6A). As the HIV RNA concentration decreases, the mean Cq and its standard deviation increase, indicating a lower number of HIV RNA targets and a higher variability in quantification. In detail, the mean Cq from the 50,000 copies/mL samples was 33.59 ± 0.30, the 5000 copies/mL samples 36.08 ± 0.70, and the 500 copies/mL 40.83 ± 0.86 (Figure 6B). As shown in Figure 6C, these mean Cqs were significantly different ($P < 0.0001$) from one of the 0 copies/mL negative controls (calculated as 50 ± 0 because all 0 copies/mL negative controls failed to amplify and yield Cq by cycle 50). Our 500 HIV RNA copies/mL LOD is lower than the 800–1000 HIV RNA copies/mL LOD of the m-PIMA system from Abbott,

which uses a similar plasma volume (50 μL of plasma).[4] The Cepheid's GeneXpert system has a LOD of 40 HIV RNA copies/mL but uses 1 mL of plasma.[4] Should the Cepheid system also use 50 μL of plasma, one would expect a theoretical LOD of 800 HIV RNA copies/mL. In addition, both m-PIMA and GeneXpert systems require plasma as the starting sample. Separating plasma from blood at the POC is challenging. Our method includes an approach for plasma separation from blood using a small and low-cost 3D-printed device. The device was able to process 100 μL of blood (with the potential for higher volumes) with 96% separation efficiency, has small device-to-device variation (Figure S8), and does not require power to operate, making it suitable for plasma separation at the POC. Compared to isothermal amplification-based methods,[36–38] our method has a higher quantitative accuracy with an R^2 of 0.97 (Figure 6B). Despite its high quantitative accuracy, our method does not require bulky and expensive equipment. In addition, the instrument completes 50 cycles of PCR in just 15 min, making it suitable for rapid quantitative NAT at the POC. Regarding the turnaround time of the entire workflow, our method takes ~45 min, which is faster than the methods discussed above.

We see several areas that require improvements. First, the plasma separation step requires some manual handling from user, which is not ideal for POC applications. A plasma separation approach that can be automated and integrated into a cartridge and therefore does not require user's intervention or requires minimal user's intervention would be better. Second, our instrument currently does not have an active bead mixing mechanism. Therefore, during the lysis/binding step, the mixture of lysis/binding buffer, magnetic beads, and the obtained plasma had to be incubated off cartridge under shaking for HIV RNA capturing before being loaded into a cartridge for bead washing, elution, and RT-PCR. If directly loading the mixture into a cartridge, the magnetic beads would settle quickly in the sample well due to their relatively large size, reducing HIV RNA capture efficiency. Using smaller magnetic beads that can stay in solution longer and/or adding active bead mixing mechanism to the instrument would enable the lysis/binding step to be implemented on a cartridge, eliminating the need of off-cartridge incubation under shaking.

CONCLUSIONS

We have reported a rapid POC HIV VL quantification method from blood with a LOD of 500 HIV RNA copies/mL. The method includes a plasma separation step using a small, power-free, 3D-printed device. With the device, we were able to separate plasma from 100 μL of blood with 96% separation efficiency. Upon the elution step, plasma solution was collected from which HIV RNA was extracted and quantified using a portable and low-cost magnetofluidic real-time RT-PCR instrument. We showed that our alcohol-free, cartridge-compatible HIV RNA extraction protocol based on PEG washing had comparable performance with two popular commercial kits. We also showed that, during the washing step in a cartridge, the washing round trip number was important to the washing efficiency. Upon tuning the number of washes, we used the platform to achieve a LOD of 500 HIV RNA copies/mL, which is below the WHO's virological failure threshold, by using 100 μL of whole blood as the starting sample, i.e., 50 HIV RNA copies in absolute copy number. Furthermore, our method had an R^2 of 0.97 upon linear fitting the standard curve, making it more accurate than isothermal amplification-based approaches, which are often

semiquantitative. In the future, we plan to add an internal control to ensure accuracy and to integrate the plasma separation step with the HIV RNA extraction and quantification step into a single cartridge to streamline the procedure and make the device truly sample-in-answer-out, which is highly desirable for POC applications.

Supplementary Material

Refer to Web version on PubMed Central for supplementary material.

ACKNOWLEDGMENTS

This work was supported by funding through the National Institutes of Health (R01AI138978, R01AI137272, and R61AI154628).

REFERENCES

(1). UNAIDS. Global HIV & AIDS statistics — Fact sheet. https://www.unaids.org/en/resources/fact-sheet ().

(2). UNAIDS. Proc. Natl. Acad. Sci. U. S. A. 2022, 119, e2117630119. [PubMed: 35042816]

(3). Cho A; Gaebler C; Olveira T; Ramos V; Saad M; Lorenzi JCC; Gazumyan A; Moir S; Caskey M; Chun TW; Nussenzweig MC Proc. Natl. Acad. Sci. U. S. A. 2022, 119, e2117630119. [PubMed: 35042816]

(4). Drain PK; Dorward J; Bender A; Lillis L; Marinucci F; Sacks J; Bershteyn A; Boyle DS; Posner JD; Garrett N Clin. Microbiol. Rev. 2019, 32, e00097. [PubMed: 31092508]

(5). NIH: National Institute of Allergy and Infectious Diseases. HIV Undetectable=Untransmittable (U=U), or Treatment as Prevention. https://www.niaid.nih.gov/diseases-conditions/treatment-prevention ().

(6). UNAIDS. Undetectable = Untransmittable. https://www.unaids.org/en/resources/presscentre/featurestories/2018/july/undetectable-untransmittable ().

(7). Rodger AJ; Cambiano V; Phillips AN; Bruun T; Raben D; Lundgren J; Vernazza P; Collins S; Degen O; Corbelli GM; Estrada V; Geretti AM; Beloukas A; Beloukas A; Coll P; Antinori A; Nwokolo N; Rieger A; Prins JM; Blaxhult A; Weber R; Van Eeden A; Brockmeyer NH; Clarke A; del Romero Guerrero J; Raffi F; Bogner JR; Wandeler G; Gerstoft J; Gutiérrez F; Brinkman K; Kitchen M; Ostergaard L; Leon A; Ristola M; Jessen H; Stellbrink HJ; Coll P; Cobarsi P; Nieto A; Meulbroek M; Carrillo A; Saz J; Guerrero JDR; García MV; Gutiérrez F; Masiä M; Robledano C; Leon A; Leal L; Redondo EG; Estrada VP; Marquez R; Sandoval R; Viciana P; Espinosa N; Lopez-Cortes L; Podzamczer D; Tiraboschi J; Morenilla S; Antela A; Losada E; Nwokolo N; Sewell J; Clarke A; Kirk S; Knott A; Rodger AJ; Fernandez T; Gompels M; Jennings L; Ward L; Fox J; Lwanga J; Lee M; Gilson R; Leen C; Morris S; Clutterbuck D; Brady M; Asboe D; Fedele S; Fidler S; Brockmeyer N; Potthoff A; Skaletz-Rorowski A; Bogner J; Seybold U; Roider J; Jessen H; Jessen A; Ruzicic S; Stellbrink HJ; Kümmerle.; Lehmann C; Degen O; Bartel S; Hüfner A; Rockstroh J; Mohrmann K; Boesecke C; Krznaric I; Ingiliz P; Weber R; Grube C; Braun D; Günthard H; Wandeler G; Furrer H; Rauch A; Vernazza P; Schmid P; Rasi M; Borso D; Stratmann M; Caviezel O; Stoeckle M; Battegay M; Tarr P; Christinet V; Jouinot F; Isambert C; Bernasconi E; Bernasconi B; Gerstoft J; Jensen LP; Bayer AA; Yehdego Y; Bach A; Handberg P; Kronborg G; Pedersen S. s.; Bülow N; Ramskover B; Ristola M; Debnam O; Sutinen J; Blaxhult A; Ask R; Hildingsson-Lundh B; Westling K; Frisen EM; Cortney G; O'Dea S; De Wit S; Necsoi C; Vandekerckhove L; Goffard JC; Henrard S; Prins J; Nobel HH; Weijsenfeld A; Van Eeden A; Elsenburg L; Brinkman K; Vos D; Hoijenga I; Gisolf E; Van Bentum P; Verhagen D; Raffi F; Billaud E; Ohayon M; Gosset D; Fior A; Pialoux G; Thibaut P; Chas J; Leclercq V; Pechenot V; Coquelin V; Pradier C; Breaud S; Touzeau-Romer V; Rieger A; Kitchen Maria Geit M; Sarcletti M; Gisinger M; Oellinger A; Menichetti S; Bini T; Mussini C; Meschiari M; Di Biagio A; Taramasso L; Celesia BM; Gussio M; Janeiro N Lancet 2019, 393, 2428–2438. [PubMed: 31056293]

(8). Eisinger RW; Dieffenbach CW; Fauci AS JAMA 2019, 321, 451–452. [PubMed: 30629090]

(9). Lecher SL; Fonjungo P; Ellenberger D; Toure CA; Alemnji G; Bowen N; Basiye Frank; Beukes A; Carmona S; De Klerk M; Diallo K; Dziuban E; Kiyaga C; Mbah H; Mengistu J; Motsoane T; Mwangi C; Mwangi JW; Mwasekaga M; Ntale J; Naluguza M; Ssewanyana I; Stevens W; Zungu I; Bhairavabhotla R; Chun H; Gaffga N; Jadczak S; Lloyd S; Nguyen S; Pati R; Sleeman K; Zeh C; Zhang G; Alexander H HIV Viral Load Monitoring Among Patients Receiving Antiretroviral Therapy — Eight Sub-Saharan Africa Countries, 2013–2018. Morb. Mortal. 2021, 70 (21), 775, DOI: 10.1056/NEJMoa1105243.

(10). World Health Organization. Consolidated guidelines on the use of antiretroviral drugs for treating and preventing HIV infection (2016). https://www.who.int/publications/i/item/9789241549684 ().

(11). World Health Organization. What's new in treatment monitoring: viral load and CD4 testing. https://www.who.int/publications/i/item/WHO-HIV-2017.22 ().

(12). Ford N; Meintjes G; Pozniak A; Bygrave H; Hill A; Peter T; Davies MA; Grinsztejn B; Calmy A; Kumarasamy N; Phanuphak P; DeBeaudrap P; Vitoria M; Doherty M; Stevens W; Siberry GK Lancet Infect. Dis. 2015, 15, 241–247. [PubMed: 25467647]

(13). Rice B; Boulle A; Schwarcz S; Shroufi A; Rutherford G; Hargreaves J JMIR Public Heal. Surveill. 2019, 5, e11136.

(14). Margot N; Koontz D; McCallister S; Mellors JW; Callebaut CJ Clin. Virol. 2018, 108, 50–52.

(15). Kibirige CN; Manak M; King D; Abel B; Hack H; Wooding D; Liu Y; Fernandez N; Dalel J; Kaye S; Imami N; Jagodzinski L; Gilmour J Sci. Rep. 2022, 12, 1–16. [PubMed: 34992227]

(16). Lima VD; Wang L; Brumme C; Wu L; Montaner JSG; Harrigan PR PLoS One 2017, 12, e0171155. [PubMed: 28152073]

(17). Nash M; Huddart S; Badar S; Baliga S; Saravu K; Pai MJ Clin. Microbiol. 2018, 56, e01673.

(18). Karasi JC; Dziezuk F; Quennery L; Förster S; Reischl U; Colucci G; Schoener D; Seguin-Devaux C; Schmit JC J. Clin. Virol. 2011, 52, 181–186. [PubMed: 21813320]

(19). Mbiva F; Tweya H; Satyanarayana S; Takarinda K; Timire C; Dzangare J; Nzombe P; Apollo T; Khabo B; Mazarura EJ Glob. Infect. Dis. 2021, 13, 85.

(20). Boeke CE; Joseph J; Atem C; Banda C; Coulibaly KD; Doi N; Gunda A; Kandulu J; Kiernan B; Kingwara L; Maokola W; Maparo T; Mbaye RN; Mtumbuka E; Mziray J; Ngugi C; Nkakulu J; Nzuobontane D; Okomo Assoumo MC; Peter T; Rioja MR; Sacks JA; Simbi R; Vojnov L; Khan SA J. Int. AIDS Soc. 2021, 24, e25663. [PubMed: 33455081]

(21). Opollo VS; Nikuze A; Ben-Farhat J; Anyango E; Humwa F; Oyaro B; Wanjala S; Omwoyo W; Majiwa M; Akelo V; Zeh C; Maman D PLoS One 2018, 13, e0209778. [PubMed: 30589900]

(22). Nicholas S; Poulet E; Wolters L; Wapling J; Rakesh A; Amoros I; Szumilin E; Gueguen M; Schramm BJ Int. AIDS Soc. 2019, 22, e25387.

(23). Mwenda R; Fong Y; Magombo T; Saka E; Midiani D; Mwase C; Kandulu J; Wang M; Thomas R; Sherman J; Vojnov L Clin. Infect. Dis. 2018, 67, 701–707. [PubMed: 29490026]

(24). Gupta-Wright A; Fielding K; van Oosterhout JJ; Alufandika M; Grint DJ; Chimbayo E; Heaney J; Byott M; Nastouli E; Mwandumba HC; Corbett EL; Gupta RK Lancet HIV 2020, 7, e620–e628. [PubMed: 32890497]

(25). Drain PK; Dorward J; Violette LR; Quame-Amaglo J; Thomas KK; Samsunder N; Ngobese H; Mlisana K; Moodley P; Donnell D; Barnabas RV; Naidoo K; Abdool Karim SS; Celum C; Garrett N Lancet HIV 2020, 7, e229–e237. [PubMed: 32105625]

(26). Mukherjee S; Cohn J; Ciaranello AL; Sacks E; Adetunji O; Chadambuka A; Mafaune H; Makayi M; McCann N; Turunga EJ Acquir. Immune Defic. Syndr. 2020, 84, S63–S69.

(27). Bwana P; Ageng'o J; Danda J; Mbugua J; Handa A; Mwau. J. Clin. Virol. 2019, 121.

(28). Meggi B; Bollinger T; Zitha A; Mudenyanga C; Vubil A; Mutsaka D; Nhachigule C; Mabunda N; Loquiha O; Kroidl A; Jani IV J. Acquir. Immune Defic. Syndr. 2021, 87, 693–699. [PubMed: 33399310]

(29). Sacks JA; Fong Y; Gonzalez MP; Andreotti M; Baliga S; Garrett N; Jordan J; Karita E; Kulkarni S; Mor O; Mosha F; Ndlovu Z; Plantier JC; Saravanan S; Scott L; Peter T; Doherty M; Vojnov L Aids 2019, 33, 1881–1889. [PubMed: 31274537]

(30). Fidler S; Lewis H; Meyerowitz J; Kuldanek K; Thornhill J; Muir D; Bonnissent A; Timson G; Frater J Sci. Rep. 2017, 7, 1–6. [PubMed: 28127051]

(31). Ehret R; Harb K; Breuer S; Obermeier MJ Clin. Virol. 2022, 149, 105127.

(32). Titchmarsh L; Zeh C; Verpoort T; Allain JP; Lee HJ Clin. Microbiol. 2015, 53, 1080–1086.

(33). Goel N; Ritchie AV; Mtapuri-Zinyowera S; Zeh C; Stepchenkova T; Lehga J; De Ruiter A; Farleigh LE; Edemaga D; So R; Sembongi H; Wisniewski C; Nadala L; Schito M; Lee HJ Virol. Methods 2017, 244, 39–45.

(34). Mauk M; Song J; Bau HH; Gross R; Bushman FD; Collman RG; Liu C Lab Chip 2017, 17, 382–394. [PubMed: 28092381]

(35). Kadimisetty K; Yin K; Roche AM; Yi Y; Bushman FD; Collman RG; Gross R; Feng L; Liu C Analyst 2021, 146, 3234–3241. [PubMed: 33999045]

(36). Phillips EA; Moehling TJ; Ejendal KFK; Hoilett OS; Byers KM; Basing LA; Jankowski LA; Bennett JB; Lin LK; Stanciu LA; Linnes JC Lab Chip 2019, 19, 3375–3386. [PubMed: 31539001]

(37). Liu T; Choi G; Tang Z; Kshirsagar A; Politza AJ; Guan W Biosens. Bioelectron. 2022, 209, 114255. [PubMed: 35429770]

(38). Hull IT; Kline EC; Gulati GK; Kotnik JH; Panpradist N; Shah KG; Wang Q; Frenkel L; Lai J; Stekler J; Lutz BR Anal. Chem. 2022, 94, 1011–1021. [PubMed: 34920665]

(39). Wang J; Kreutz JE; Thompson AM; Qin Y; Sheen AM; Wang J; Wu L; Xu S; Chang M; Raugi DN; Smith RA; Gottlieb GS; Chiu DT Lab Chip 2018, 18, 3501–3506. [PubMed: 30351338]

(40). Trick AY; Ngo HT; Nambiar AH; Morakis MM; Chen F-E; Chen L; Hsieh K; Wang T-H Lab Chip 2022, 22, 945–953. [PubMed: 35088790]

(41). Macdonald J; Von Stetten F; Li J Analyst 2019, 144, 31.

(42). Jones L; Naikare HK; Mosley YYC; Tripp RA BioTechniques 2022, 72, 263–272. [PubMed: 35545967]

(43). Mendoza-Gallegos RA; Rios A; Garcia-Cordero JL Anal. Chem. 2018, 90, 5563–5568. [PubMed: 29624373]

(44). Shin DJ; Trick AY; Hsieh YH; Thomas DL; Wang TH Sci. Rep. 2018, 8, 1–12. [PubMed: 29311619]

(45). Trick AY; Melendez JH; Chen FE; Chen L; Onzia A; Zawedde A; Nakku-Joloba E; Kyambadde P; Mande E; Matovu J; Atuheirwe M; Kwizera R; Gilliams EA; Hsieh YH; Gaydos CA; Manabe YC; Hamill MM; Wang TH Sci. Transl. Med. 2021, 13, 6356.

(46). Ngo HL; Nguyen HD; Tran VN; Ngo HT IFMBE Proc. 2022, 85, 69–83.

(47). Qiu X; Ge S; Gao P; Li K; Yang Y; Zhang S; Ye X; Xia N; Qian S SLAS Technol. 2017, 22, 13–17. [PubMed: 27272156]

(48). World Health Organization. Guidelines for managing advanced HIV disease and rapid initiation of antiretroviral therapy. https://www.who.int/publications/i/item/9789241550062 ().

(49). Qin S; Lai J; Zhang H; Wei D; Lv Q; Pan X; Huang L; Lan K; Meng Z; Liang H; Ning C BMC Infect. Dis. 2021, 21, 1–11. [PubMed: 33390160]

(50). Palmer S; Wiegand AP; Maldarelli F; Bazmi H; Mican JAM; Polis M; Dewar RL; Planta A; Liu S; Metcalf JA; Mellors JW; Coffin JM J. Clin. Microbiol. 2003, 41, 4531–4536. [PubMed: 14532178]

(51). Scallan MF; Dempsey C; Macsharry J; O'callaghan I; O'connor PM; Horgan CP; Durack E; Cotter PD; Hudson S; Moynihan HA; Lucey B Validation of a Lysis Buffer Containing 4 M Guanidinium Thiocyanate (GITC)/ Triton X-100 for Extraction of SARS-CoV-2 RNA for COVID-19 Testing: Comparison of Formulated Lysis Buffers Containing 4 to 6 M GITC, Roche External Lysis Buffer and Qiagen RTL Lysis Buffer. BioRxiv 2020.

(52). Robinson M; Marks H; Hinsdale T; Maitland K; Coté G Biomicrofluidics 2017, 11, 024109. [PubMed: 28405258]

(53). Guo W; Hansson J; Van Der Wijngaart W Anal. Chem. 2020, 92, 6194–6199. [PubMed: 32323979]

(54). Liu CH; Chen CA; Chen SJ; Tsai TT; Chu CC; Chang CC; Chen CF Anal. Chem. 2019, 91, 1247–1253. [PubMed: 30537809]

(55). Hauser J; Lenk G; Hansson J; Beck O; Stemme G; Roxhed N Anal. Chem. 2018, 90, 13393–13399. [PubMed: 30379058]

(56). Baillargeon KR; Murray LP; Deraney RN; Mace CR Anal. Chem. 2020, 92, 16245–16252. [PubMed: 33227204]

(57). Nabatiyan A; Parpia ZA; Elghanian R; Kelso DM J. Virol. Methods 2011, 173, 37–42. [PubMed: 21219933]

(58). Vemulapati S; Erickson D Anal. Chem. 2019, 91, 14824–14828. [PubMed: 31738522]

(59). Liu C; Liao SC; Song J; Mauk MG; Li X; Wu G; Ge D; Greenberg RM; Yang S; Bau HH Lab Chip 2016, 16, 553–560. [PubMed: 26732765]

(60). Zhang H; Anoop K; Huang C; Sadr R; Gupte R; Dai J; Han A Sens. Actuators, B 2022, 354, 131180.

(61). Kim CH; Park J; Kim SJ; Ko DH; Lee SH; Lee SJ; Park JK; Lee MK Sens. Actuators, B 2020, 320, 128346.

(62). Park BH; Oh SJ; Jung JH; Choi G; Seo JH; Kim DH; Lee EY; Seo TS Biosens. Bioelectron. 2017, 91, 334–340. [PubMed: 28043075]

(63). Berry SM; Alarid ET; Beebe DJ Lab Chip 2011, 11, 1747–1753. [PubMed: 21423999]

(64). Paul R; Ostermann E; Wei Q Biosens. Bioelectron. 2020, 169, 112592. [PubMed: 32942143]

(65). Yin J; Suo Y; Zou Z; Sun J; Zhang S; Wang B; Xu Y; Darland D; Zhao JX; Mu Y Lab Chip 2019, 19, 2769–2785. [PubMed: 31365009]

(66). Pearlman SI; Leelawong M; Richardson KA; Adams NM; Russ PK; Pask ME; Wolfe AE; Wessely C; Haselton FR ACS Appl. Mater. Interfaces 2020, 12, 12457–12467. [PubMed: 32039572]

(67). Liu W; Yue F; Lee LP Acc. Chem. Res 2021, 54, 23.

(68). Wen J; Legendre LA; Bienvenue JM; Landers JP Purification of Nucleic Acids in Microfluidic Devices The Functionality of Micropillars, Microposts, Silica Beads, Silica Particles, Sol-Gels, and Porous Monoliths Provides a Framework for Sample Preparation and Analysis for an Integrated Microfluidic System, DOI: 10.1021/ac8014998.

(69). Chen Y; Liu Y; Shi Y; Ping J; Wu J; Chen H TrAC - Trends Anal. Chem. 2020, 127, 115912.

(70). Li Z; Bai Y; You M; Hu J; Yao C; Cao L; Xu F Biosens. Bioelectron. 2021, 177, 112952. [PubMed: 33453463]

(71). Shin DJ; Athamanolap P; Chen L; Hardick J; Lewis M; Hsieh YH; Rothman RE; Gaydos CA; Wang TH Sci. Rep. 2017, 7, 1–10. [PubMed: 28127051]

(72). Chen FE; Lee PW; Trick AY; Park JS; Chen L; Shah K; Mostafa H; Carroll KC; Hsieh K; Wang TH Biosens. Bioelectron. 2021, 190, 113390. [PubMed: 34171821]

(73). Shi X; Chen C-H; Gao W; Chao S-H; Meldrum DR From Chip-in-a-Lab to Lab-on-a-Chip: Towards a Single Handheld Electronic System for Multiple Application-Specific Lab-on-a-Chip (ASLOC). 2015, 15, 1059, DOI: 10.1039/c4lc01111b.

(74). Choi G; Prince T; Miao J; Cui L; Guan W Biosens. Bioelectron. 2018, 115, 83–90. [PubMed: 29803865]

(75). Strotman LN; Lin G; Berry SM; Johnson EA; Beebe DJ Analyst 2012, 137, 4023–4028. [PubMed: 22814365]

(76). Psifidi A; Dovas CI; Bramis G; Lazou T; Russel CL; Arsenos G; Banos G PLoS One 2015, 10, e0115960. [PubMed: 25635817]

(77). Yin J; Zou Z; Hu Z; Zhang S; Zhang F; Wang B; Lv S; Mu Y Lab on a Chip A “Sample-in-Multiplex-Digital-Answer-out” Chip for Fast Detection of Pathogens †. 2020, 20, 979, DOI: 10.1039/c9lc01143a.

(78). Yin J; Hu J; Sun J; Wang B; Mu Y Analyst 2019, 144, 7032. [PubMed: 31651914]

(79). Mosley O; Melling L; Tarn MD; Kemp C; Esfahani MMN; Pamme N; Shaw KJ Lab Chip 2016, 16, 2108–2115. [PubMed: 27164181]

(80). Juang DS; Juang TD; Dudley DM; Newman CM; Accola MA; Rehrauer WM; Friedrich TC; O’Connor DH; Beebe DJ Nat. Commun. 2021, 12, 1. [PubMed: 33397941]

(81). Trick AY; Chen FE; Chen L; Lee PW; Hasnain AC; Mostafa HH; Carroll KC; Wang TH Adv. Mater. Technol. 2022, 7, 2101013. [PubMed: 35441089]

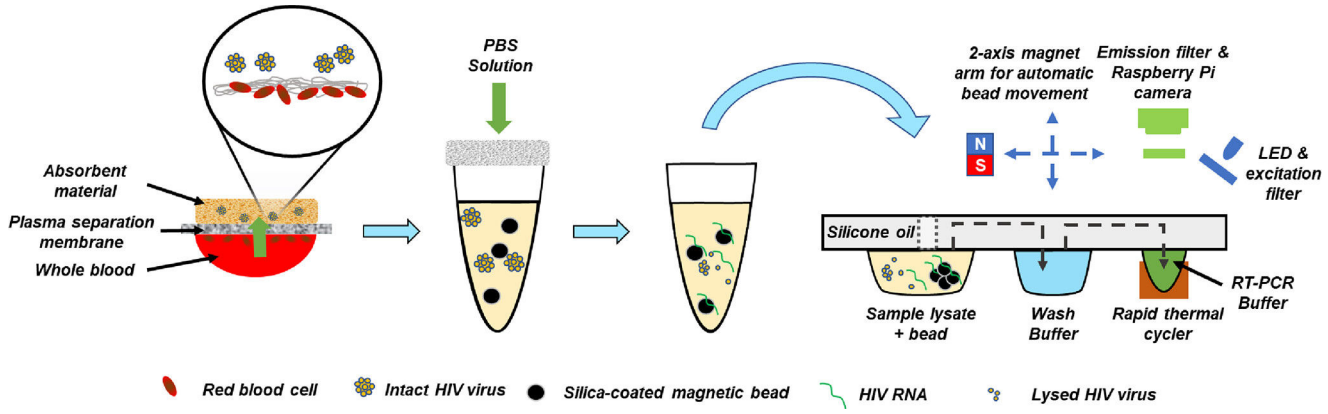

Figure 1.

Working principle of the proposed POC HIV VL quantification method. First, plasma is separated from blood by a device composed of a plasma separation membrane and an absorbent material. Second, a flow of PBS is used to elute the absorbed plasma into a lysis/binding buffer containing silica-coated magnetic beads for HIV virus lysing and HIV RNA capturing. Finally, the solution is transferred into a cartridge for automatic washing, elution, and quantification using a portable magnetofluidic real-time RT-PCR instrument.

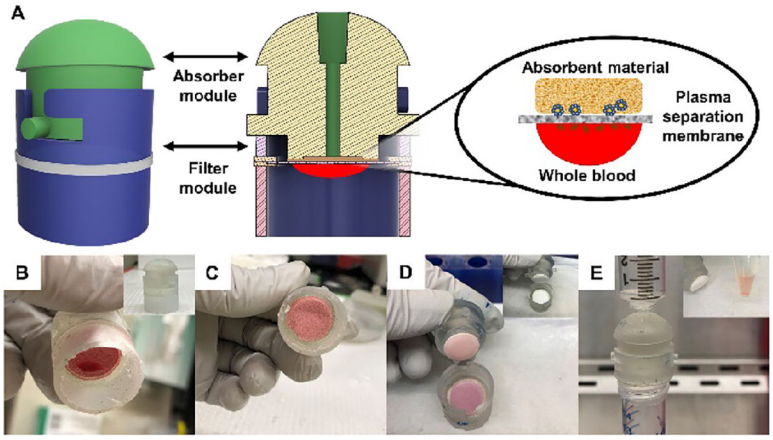

Figure 2.

(A) Working principle of the plasma separation device. The absorber module, which holds the absorbent material, is twist-and-locked with the filter module, which holds the plasma separation membrane. Thus, the absorbent material receives flush contact with the plasma separation membrane. Upon loading with blood, red blood cells are trapped by the plasma separation membrane, whereas plasma and viruses are absorbed into the absorbent material on the other side of the membrane. Result: (B) Blood was loaded onto the bottom surface of the plasma separation membrane. (C) The membrane appeared dry after 3 min because plasma was absorbed into the absorbent material on the other side. (D) The absorber module with the absorbent material was detached from the filter module. (E) Plasma in the absorbent material was eluted into a collection tube using a syringe loaded with PBS.

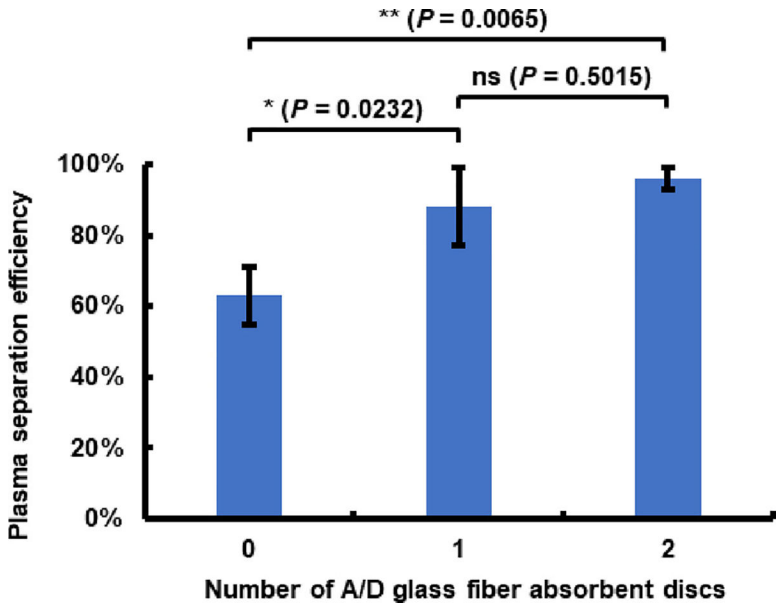

Figure 3.

Plasma separation efficiency depends on the absorbent capacity. When a blotting paper absorbent disc was combined with the increasing numbers of A/D glass fiber absorbent discs (0, 1, and 2), the plasma separation efficiency increased (63, 88, and 96%, respectively). The error bars represent the standard deviation ($n = 3$). ns stands for nonsignificant.

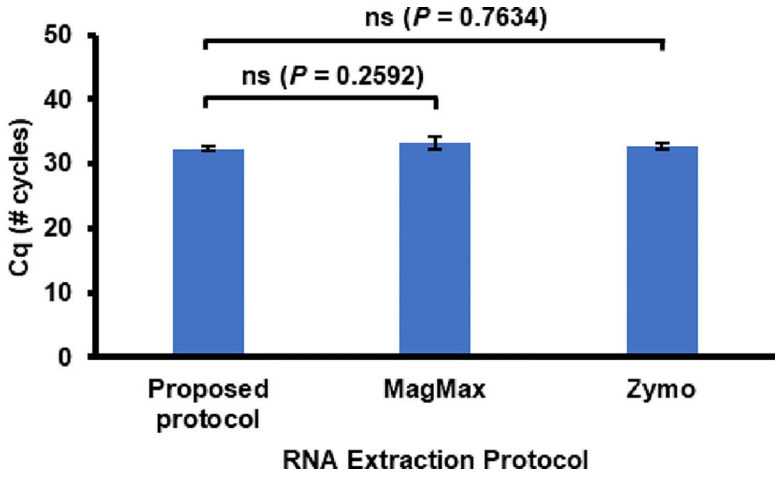

Figure 4.

Comparison between our proposed RNA extraction protocol and MagMAX Viral RNA Isolation Kit and Zymo Quick-DNA/RNA Viral MagBead commercial kits. Student *t*-tests showed no significant difference between Cq of our protocol and Cq of the two commercial kits. The error bars represent the standard deviation ($n = 3$). ns stands for nonsignificant.

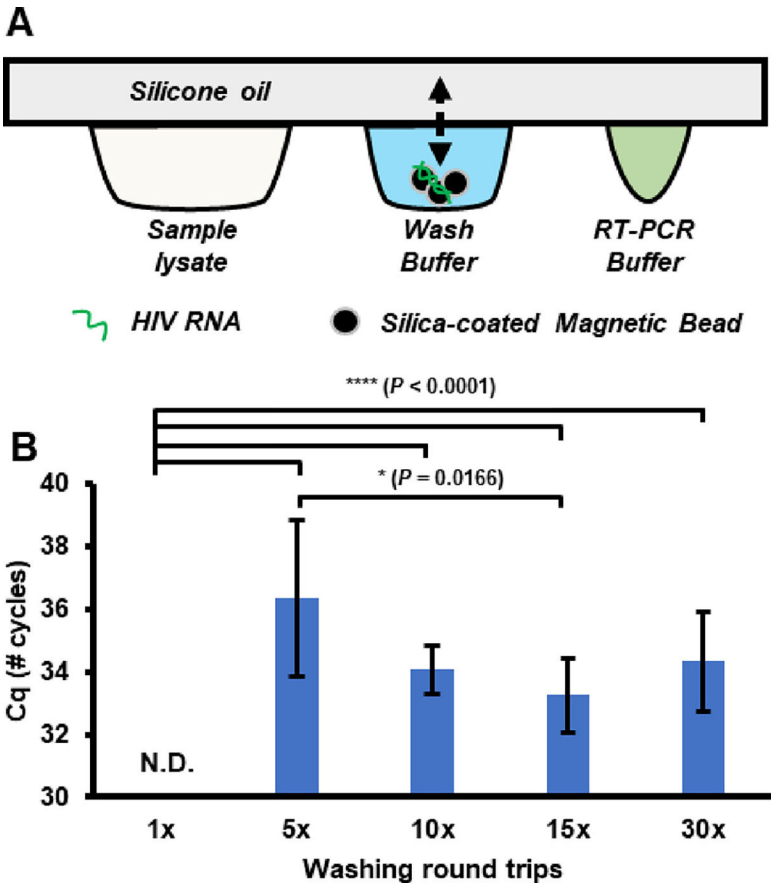

Figure 5.

(A) Silica-coated magnetic beads with HIV RNA bound on their surface were moved down and up between the washing buffer and the silicone oil repeated times to improve washing efficiency. (B) With just 1 washing round trip, no Cq was detected. With more washing round trips, Cq decreased, reaching the lowest at 15 washing round trips, before increasing again at 30 washing round trips. The error bars represent the standard deviation ($n = 3$). N.D. stands for non-detected.

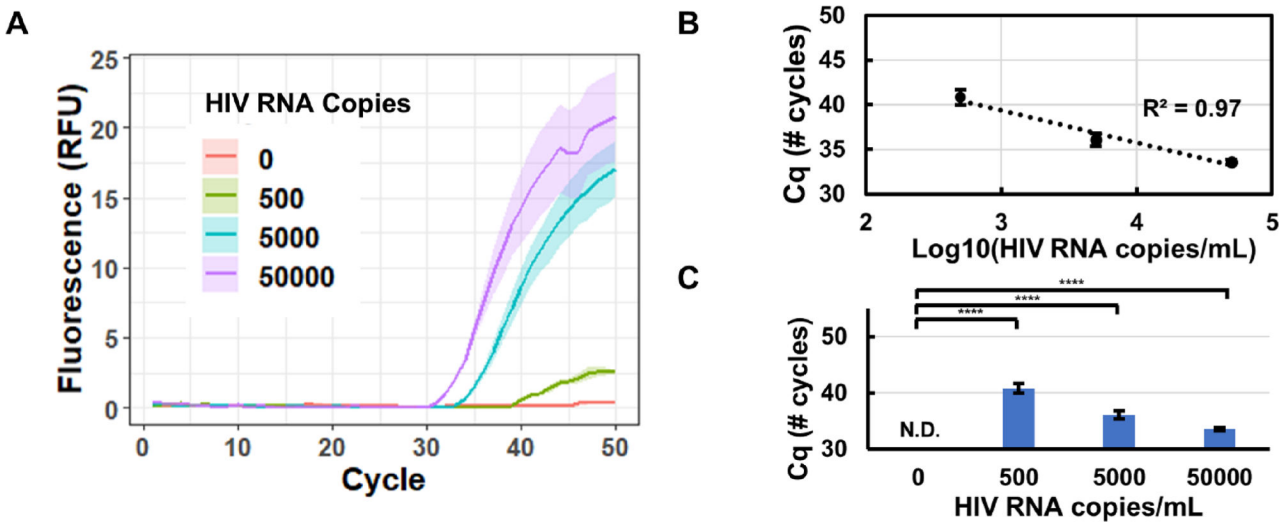

Figure 6.

Calibration curve. A finger-prick volume of blood (100 μL) spiked with HIV viral particles with 50,000 HIV RNA copies/mL, 5000 HIV RNA copies/mL, 500 HIV RNA copies/mL, and 0 HIV RNA copies/mL final concentrations was loaded onto our plasma separation device for plasma separation, followed by automatic HIV RNA extraction and ultrafast real-time RT-PCR-based quantification in magnetofluidic cartridges. Amplification curves (A) and Cq values (B) could still be observed and calculated at 500 HIV RNA copies/mL. The shaded area represents the 95% prediction band, where 95% of future samples are expected to fall. The error bars represent the standard deviation ($n = 3$). N.D. stands for non-detected. **** indicates $P < 0.0001$.